Separation Science and Technology
Publication details, including instructions for authors and subscription information:
http://www.informaworld.com/smpp/title~content=t713708471

Measurement of the Hydraulic Permeability of Microporous Membranes from the Streaming Potential Decay

A. Hernández[a]; J. I. Calvo[a]; L. Martínez[a]; J. A. Ibáñez[a]; F. Tejerina[a]
[a] Departamento Fisica Aplicada II, Universidad De Valladolid, Valladolid, Spain

To cite this Article Hernández, A. , Calvo, J. I. , Martínez, L. , Ibáñez, J. A. and Tejerina, F.(1991) 'Measurement of the Hydraulic Permeability of Microporous Membranes from the Streaming Potential Decay', Separation Science and Technology, 26: 12, 1507 — 1517

To link to this Article: DOI: 10.1080/01496399108050547

URL: http://dx.doi.org/10.1080/01496399108050547

SEPARATION SCIENCE AND TECHNOLOGY, 26(12), pp. 1507–1517, 1991

Measurement of the Hydraulic Permeability of Microporous Membranes from the Streaming Potential Decay

---

A. HERNÁNDEZ, J. I. CALVO, L. MARTÍNEZ, J. A. IBÁÑEZ, and F. TEJERINA
DEPARTAMENTO FISICA APLICADA II
UNIVERSIDAD DE VALLADOLID
47071 VALLADOLID, SPAIN

Abstract

The standard methods used to measure the hydraulic permeability of microporous membranes are revised. It is proposed that the relaxation of the streaming potential be used once an initial pressure difference is established and the system is free to evolve. This method is compared with those that use pressure or height decay, and its simplicity and easy automatization is pointed out. The results are compared with those obtained by measuring the volume flow for several constant pressures (as suggested by the definition) for four different Nuclepore membranes and LiCl–water solutions (1×10^{-3} mol/L) at 298.0 ± 0.5 K. These results coincide within the error range.

INTRODUCTION

When gradients of electric potential and pressure are the only generalized forces through a microporous membrane, a volume flux and an electric current can be generated according to the equations

$$\left.\begin{aligned} J_v &= L_{11}\Delta p + L_{12}\Delta\phi \\ I &= L_{21}\Delta p + L_{22}\Delta\phi \end{aligned}\right\} \qquad (1)$$

that can be obtained from the linear theory of thermodynamics of irreversible processes, i.e., for systems that are not very far from equilibrium. In Haase's formulation (*1–3*) these equations are valid for any solute and solvent, and the fluxes and gradients are directly accessible from experiments.

Any gradient or flux can be kept equal to zero and one of the others can be taken as independent in order to set up one of the electrokinetic phenomena shown in Table 1. From them, both kinds of permeation have a special relevance as regards a microporous membrane. On the other hand, Onsager's reciprocity equations (*3,4*) are fully applicable to these phenomena. Therefore, the cross phenomenological coefficients are equal to each other ($L_{12} = L_{21}$).

Two permeation coefficients can be defined. The first-class permeation coefficient is

$$(J_v/\Delta p)_{\Delta\phi=0} = L_{11} \tag{2}$$

and the second-class permeation coefficient or hydraulic permeability is

$$(J_v/\Delta p)_{I=0} = \lambda_p = \left(L_{11} - \frac{L_{12}L_{21}}{L_{22}}\right) \tag{3}$$

TABLE 1
Classification of Electrokinetic Phenomena

$J_v = 0$	$\Delta P = -\frac{L_{12}}{L_{11}}\Delta\phi$	Electroosmotic pressure
	$I = \left(L_{22} - \frac{L_{12}L_{21}}{L_{11}}\right)\Delta\phi$	Second-class conduction
	$I = \left(L_{21} - \frac{L_{22}L_{11}}{L_{12}}\right)\Delta P$	
$I = 0$	$\Delta\phi = -\frac{L_{12}}{L_{22}}\Delta P$	Streaming potential
	$J_v = \left(L_{11} - \frac{L_{21}L_{12}}{L_{22}}\right)\Delta P$	Second class permeation
	$J_v = \left(L_{12} - \frac{L_{22}L_{11}}{L_{21}}\right)\Delta\phi$	
$\Delta P = 0$	$J_v = L_{12}\Delta\phi$	Electroosmosis
	$I = L_{22}\Delta\phi$	Conduction
	$J_v = (L_{12}/L_{22})I$	
$\Delta\phi = 0$	$J_v = L_{11}\Delta P$	Permeation
	$I = L_{21}\Delta P$	Streaming current
	$J_v = (L_{11}/L_{12})I$	

It is clear that in a typical permeation experiment, no circuit is closed; therefore, there is no electric current through the liquid phases in the stationary state. Of course, when a nonelectrolyte is used as the solute, there is almost no electric potential difference, but this is only due to the extremely low value of L_{12}. And, in those systems, the permeation coefficients are close to being equal. Thus, it is λ_p, the permeability, that is usually found to relate volume flux and pressure gradient in permeation. It would be difficult to establish the nonpotential condition, because it would be necessary to short circuit two electrodes placed in contact with the membrane.

Several methods have been proposed in order to measure hydraulic permeability. First, the definition given by Eq. (3) suggests keeping Δp constant and measuring J_v. If this is done for several values of Δp, a straight line is obtained whose slope is λ_p. This is a very boring and bothersome process because it is difficult to reproduce the same experimental conditions exactly through all the steps of the method.

Some more elaborate methods have been proposed (*5–8*) in which the pressure decay is followed once the system becomes free to evolve. In order to take benefit of the ease and simplicity of measurement, registration, and automatic handling of an electric signal, these methods can be transformed in order to use the decay of the electric potential that arises when any pressure gradient is present. Here, this streaming potential decay is studied and tested to measure the hydraulic permeability.

THEORY

The pressure drop through the membrane can be controlled by means of two capillaries of section S placed over the phases at each side of the membrane, as shown in Fig. 1. When the system is isolated, the level difference is followed in time, and we have (*3,9*)

$$J_v = -\frac{S}{2}\frac{dh}{dt} \tag{4}$$

$$\Delta p = \rho g h \tag{5}$$

In zero-intensity conditions we have (see Table 1)

$$\Delta p = J_v/\lambda_p \tag{6}$$

$$\Delta\phi = J_v/\alpha_p \tag{7}$$

where

$$\alpha_p = L_{12} - \frac{L_{11}L_{22}}{L_{21}} \tag{8}$$

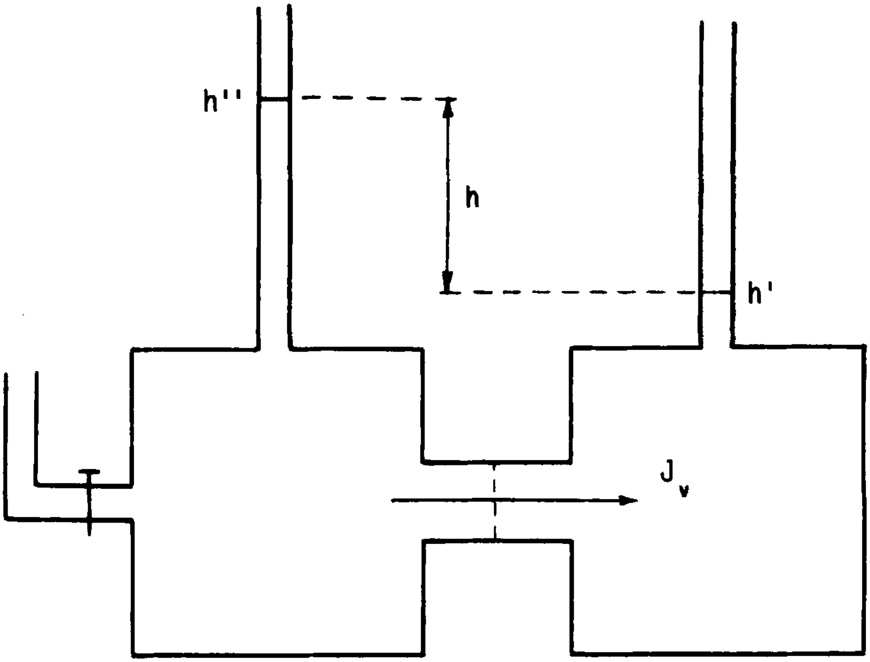

FIG. 1. Schematic representation of a typical relaxation experiment.

Therefore, from Eqs. (4), (6), and (7) we infer

$$\Delta p = -\frac{S}{2\lambda_p}\frac{dh}{dt} \tag{9}$$

$$\Delta\phi = -\frac{S}{2\alpha_p}\frac{dh}{dt} \tag{10}$$

and, by using Eqs. (5) and (9),

$$\rho g h = -\frac{S}{2\lambda_p}\frac{dh}{dt} \tag{11}$$

This can be integrated to

$$h = h_0 e^{-t/\tau_l} \tag{12}$$

where

$$\frac{1}{\tau_l} = \frac{2\rho g}{S} \lambda_p \tag{13}$$

Then, from Eqs. (6)–(10) and (4) and (12):

$$\Delta\phi = \Delta\phi_0 e^{-t/\tau_l} \tag{14}$$

$$\Delta p = \Delta p_0 e^{-t/\tau_l} \tag{15}$$

$$J_v = J_{v0} e^{-t/\tau_l} \tag{16}$$

If any of the forces or fluxes given by Eqs. (14) and (15) are followed over time and fitted to an exponential function, the relaxation time obtained can be related to the hydraulic permeability by using Eq. (13).

The liquid levels are usually followed in both capillaries and fitted to

$$h_1 = -\frac{h_0'' - h_0'}{2} e^{-t/\tau_l} \quad \text{falling capillary} \tag{17}$$

$$h_2 = +\frac{h_0'' - h_0'}{2} e^{-t/\tau_l} \quad \text{rising capillary} \tag{18}$$

that are each obtained from Eq. (12) by an origin translation.

These levels frequently move very quickly and cannot be experimentally followed. This is why a "half time" method is used, i.e., the time corresponding to

$$h_1 = h_{10}/2 = (h_0'' - h_0')/4 \tag{19}$$

is taken, $t_{0.5}$, and λ_p is obtained from Eq. (19) as

$$\lambda_p = \frac{S \ln 2}{2\rho g t_{0.5}} \tag{20}$$

In fact the same can be done with the electric potential by using Eq. (14) instead of Eq. (12) and defining $t_{0.5}$ as the time necessary for the electric potential to be reduced to half its initial value and using Eq. (20).

EXPERIMENTAL METHOD

The experimental device is schematically shown in Fig. 2. The main component is a membrane cell made of methacrylate with an approximate volume of 125×10^{-6} m^3. Each semicell is magnetically stirred and has an immersed chloride selective electrode. There is also a vertical capillary with a very uniform cross section of 6.88×10^{-6} m^2 as measured by the mercury drop method.

The high pressure semicell is connected to a Mariotte flask in order to

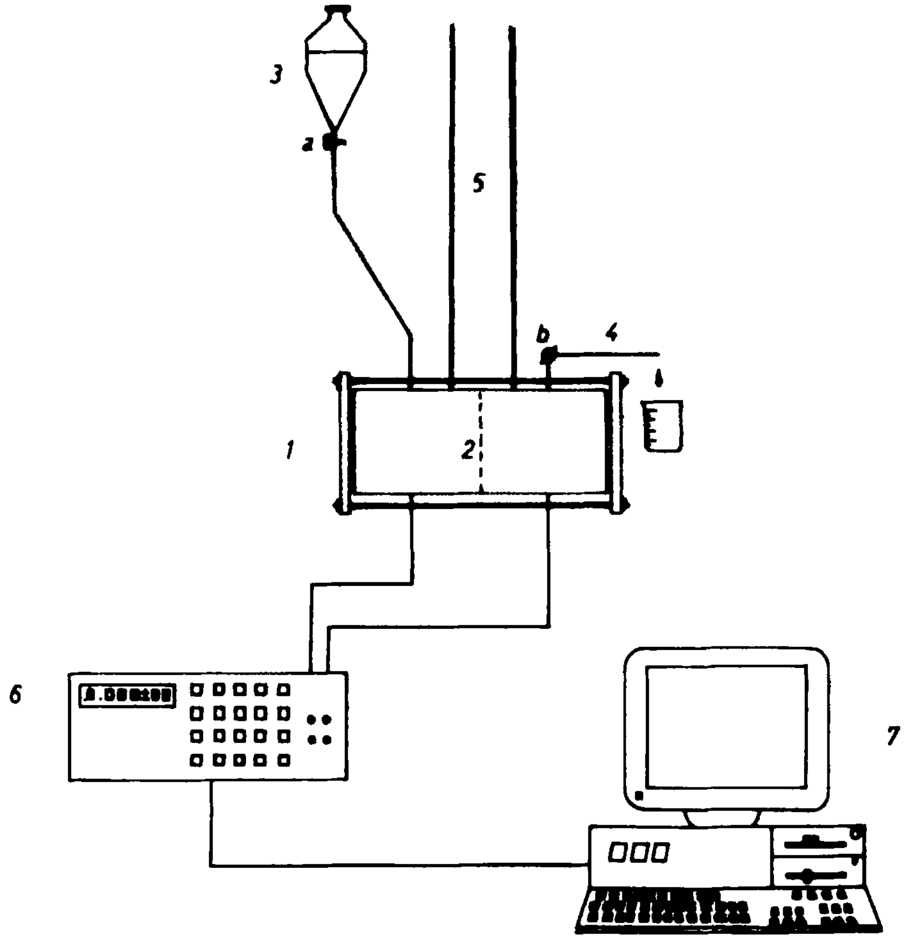

FIG. 2. Experimental device: (1) membrane cell, (2) membrane holder, (3) Mariotte flask, (4) volume flow output, (5) vertical capillaries, (6) digital voltmeter, (7) computer.

have constant pressure whenever necessary. The low pressure side has an output that allows volume flow measurement.

The electrodes are connected to a high-impedance voltmeter which is controlled by a computer.

Between the semicells there is a membrane holder, also made of methacrylate, that exposes a transport membrane area of 7.07×10^{-4} m^2.

Several Nuclepore filters, which consist of a thin sheet of polycarbonate perforated by an array of discrete and nearly parallel cylindrical pores obtained by a track-etching method, are used as membranes. Their main characteristics, according to the manufacturer's data, are shown in Table 2.

Both semicells were filled with an LiCl solution of the same concentration, 1.0×10^{-3} N, and all the experiments were conducted at 298.0 ± 0.5 K. Solutions were made from distilled de-gasified and de-ionized water and reagent grade LiCl.

A constant pressure gradient was first provided with a maximum of 30 cm of liquid column, measured by means of a cathetometer. Then the volume flow was obtained by weighting and timing, and the hydraulic permeability was related to the slope of a representation of J_v versus Δp according to Eq. (3). Each experiment was done with a new, clean membrane.

Once the maximum pressure had been established, the input and recording of data supplied by the voltmeter were started by the computer. After that, keys a and b (see Fig. 2) were closed simultaneously and the relaxation of the electric potential was registered. These data are stored and can be fitted to an exponential function of the form

$$y = ae^{-x/b} + c \tag{21}$$

by a standard nonlinear regression program that uses the Marquardt algorithm. In Eq. (21), y is the electric potential difference directly obtained

TABLE 2
Main Characteristics of the Studied Membranes According to Manufacturer's Data

Membrane	Pore size (μm)	Pore density, (pores/cm^2)	Thickness (μm)
N02	0.2	3×10^8	10
N01	0.1	3×10^8	6
N005	0.05	6×10^8	6
N003	0.03	6×10^8	6

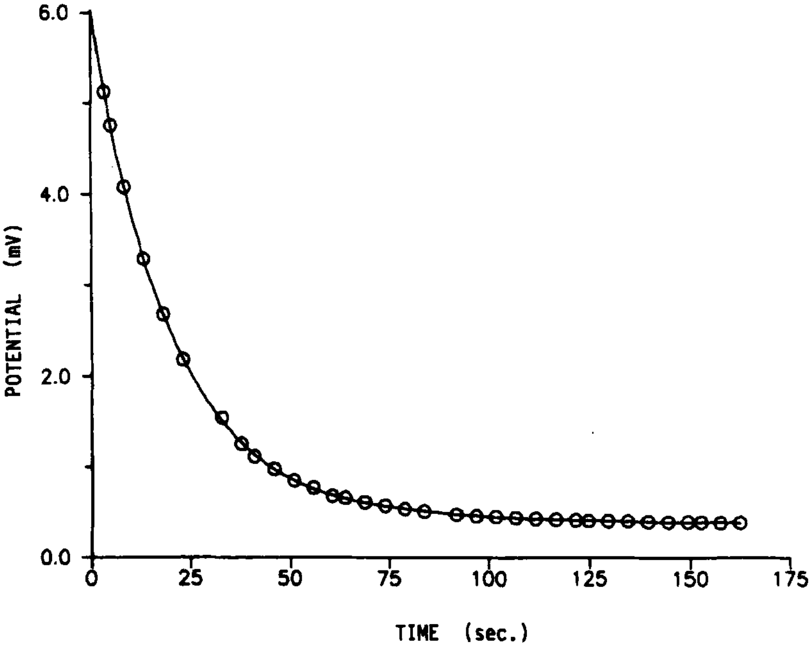

FIG. 3. Directly measured potential relaxation for N02 membrane.

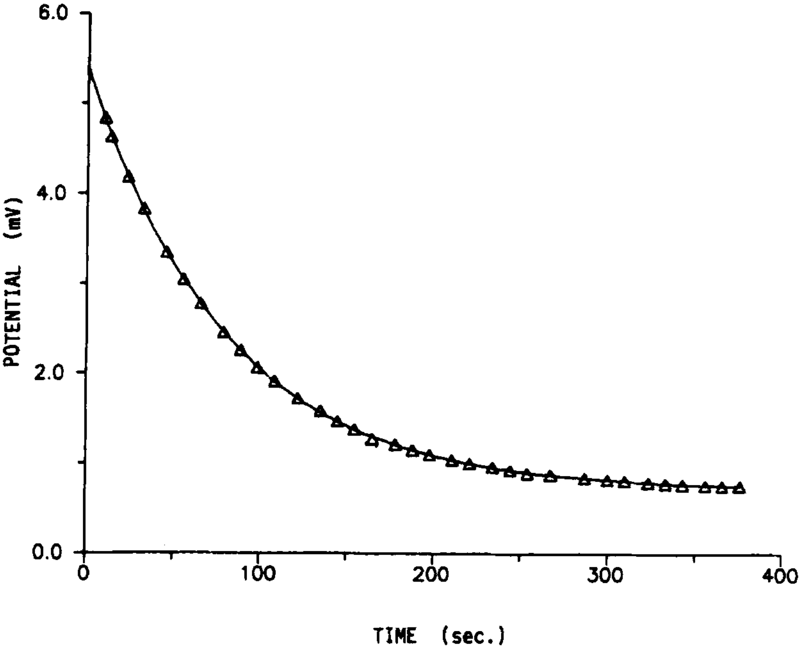

FIG. 4. Directly measured potential relaxation for N01 membrane.

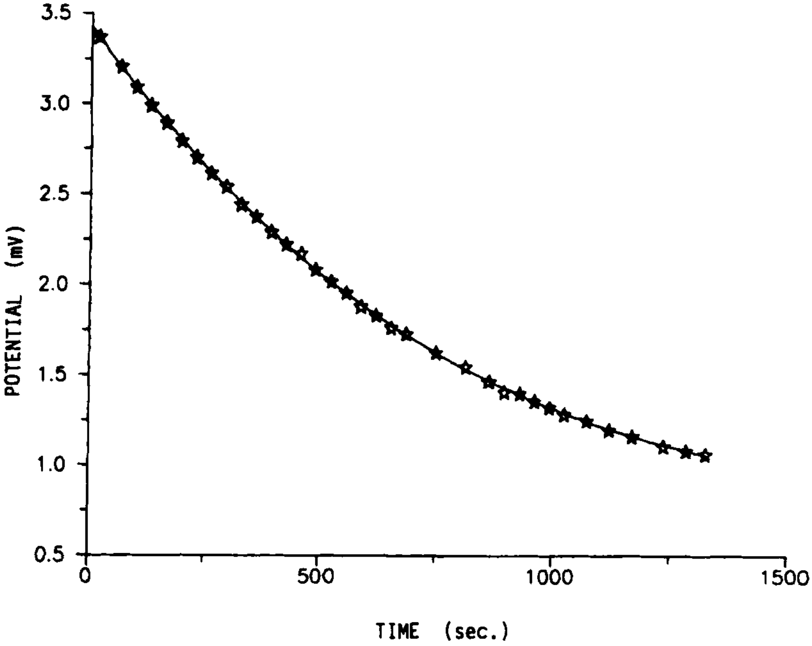

FIG. 5. Directly measured potential relaxation for N005 membrane.

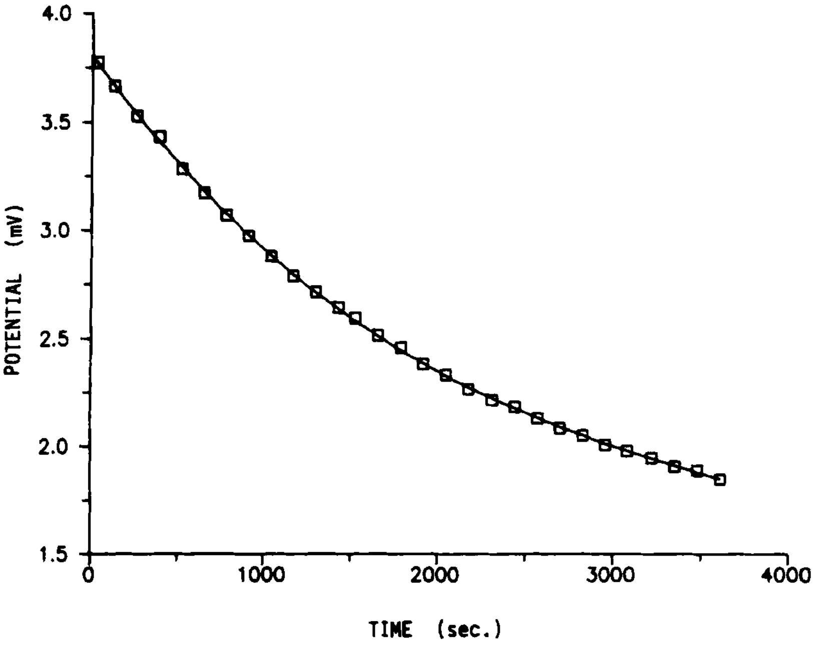

FIG. 6. Directly measured potential relaxation for N003 membrane.

TABLE 3
The Initial and Asymmetric Streaming Potentials, and the Time Necessary to Have $\Delta\phi_0/2$

Membrane	$\Delta\phi_0$ ($V \times 10^{-3}$)	$\Delta\phi_{as}$ ($V \times 10^{-3}$)	$t_{0.5}$ (s)
N02	(5.52 ± 0.42)	(0.55 ± 0.13)	14.7 ± 1.3
N01	(4.83 ± 0.23)	(0.63 ± 0.16)	54.2 ± 3.3
N005	(3.03 ± 0.42)	(0.55 ± 0.18)	506.8 ± 24.2
N003	(2.25 ± 0.25)	(0.76 ± 0.38)	1404.5 ± 179.9

from the voltmeter and c is an undesirable but unavoidable contribution due to differences between the electrodes, which is called the asymmetric potential, $\Delta\phi_{as}$. Therefore, the real streaming potential is given by $y - c$, and a and b are $\Delta\phi_0$ and $1/\tau_l$, respectively, according to Eq. (14). Finally, from Eq. (13), we obtain λ_p.

RESULTS AND CONCLUSIONS

The relaxation profiles of the directly measured potentials are shown for all the membranes studied in Figs. 3–6. The initial and asymmetric streaming potentials, $\Delta\phi_0$ and $\Delta\phi_{as}$, and $t_{0.5}$ are shown in Table 3. By taking into

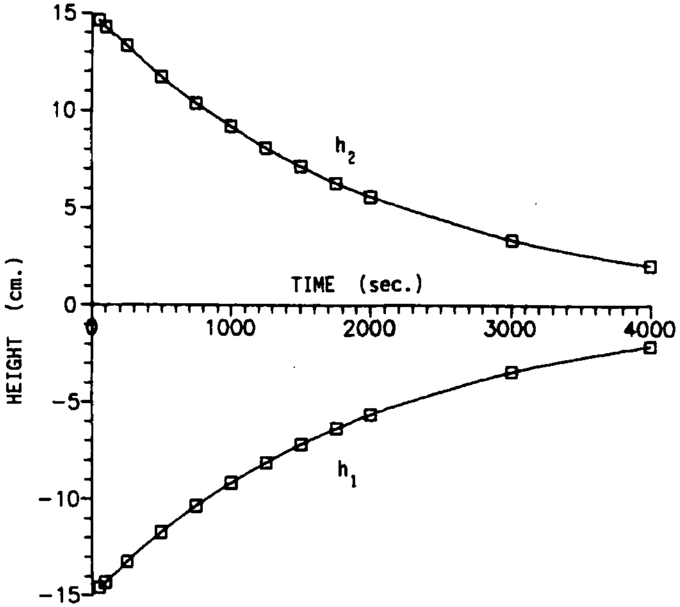

FIG. 7. h_1 and h_2 heights (defined in Eqs. 17 and 18) versus time for N003 membrane.

TABLE 4
Results for the Hydraulic Permeability Obtained from Eq. (3), λ_p (slope), and from the Streaming Potential Relaxation, λ_p (fitted)

Membrane	λ_p (fitted) ($m^3/s{\cdot}N$)	λ_p (slope) ($m^3/s{\cdot}N$)
N02	$(2.34 \pm 0.23) \times 10^{-8}$	$(3.00 \pm 0.51) \times 10^{-8}$
N01	$(6.35 \pm 0.41) \times 10^{-9}$	$(5.52 \pm 0.42) \times 10^{-9}$
N005	$(6.79 \pm 0.34) \times 10^{-10}$	$(6.20 \pm 0.23) \times 10^{-10}$
N003	$(2.45 \pm 0.36) \times 10^{-10}$	$(2.16 \pm 0.20) \times 10^{-10}$

account the values of $t_{0.5}$ in Table 3, it is clear that the height relaxation most easily followed in time corresponds to the N003 membrane, as shown in Fig. 7. The values of the hydraulic permeability obtained from Eq. (3) and from the fitting methods are shown in Table 4. Of course, the same results are given for λ_p by Eq. (12) or (13) and Eq. (14), and by Eq. (20).

All the results for hydraulic permeability are given by unit area of membrane exposed to transport in order to normalize them.

From Table 4 it is seen that the hydraulic permeability can be measured by the streaming potential relaxation as well as by the volume flow versus pressure representation, given that the values obtained are equal once the experimental errors are taken into account. In any case, the relaxation method is easier, faster, and allows for the automatic handling and storage of data.

Acknowledgments

The authors gratefully acknowledge the support of this work under CICYT Grant PA86-0219(PNICE and DT).

REFERENCES

1. R. Haase, *Z. Phys. Chem., Neue Folge, 103,* 225 (1976).
2. R. Haase, *Ibid., 103,* 235 (1976).
3. R. Haase, *Ibid., 103,* 247 (1976).
4. N. Laksminarayanaiah, *Transport Phenomena in Membranes,* Academic Press, New York, 1972.
5. T. Teorell, *J. Gen. Physiol., 42,* 831 (1959).
6. P. Meares and K. R. Page, *Philos. Trans. R. Soc., 272,* 1 (1972).
7. C. Fernández-Pineda and J. Mengual, *J. Colloid Interface Sci., 61,* 95 (1977).
8. C. Fernández-Pineda and F. Serrano, *J. Membr. Sci., 19,* 325 (1984).
9. A. Hernández, A. Martín, L. Martínez, J. A. Ibáñez, and F. Tejerina, *J. Non-Equilib. Thermodyn., 15,* 103 (1990).

Received by editor September 24, 1990